Supporting Information

Genome-Resolved Insights into Ni/Fe_2O_3 Nanocatalyst-Enhanced Dark Fermentative Hydrogen Production from Food Waste

*Puranjan Mishra [a], Ruilong Zhang [a], Peixin Wang[a], Yiqi Geng [a], Dongyi Li [ab], Qiuxiang Xu[b], Jonathan W.C. Wong [b], Jun Zhao [a,c] **

[a] Sino-Forest Applied Research Centre for Pearl River Delta Environment, Department of Biology, Hong Kong Baptist University, Hong Kong, China

[b] Research Center for Eco-Environmental Engineering, Dongguan University of Technology, Dongguan, Guangdong 523808, China

[c] Institute of Advanced Materials, Hong Kong Baptist University, Hong Kong, China

* Corresponding author: Jun Zhao: zhaojun@hkbu.edu.hk

Section 1. Food waste preparation

Bread (35%), Cabbage (25%), Rice (25%) and cooked meat 15% on a wet-weight basis as per Chakraborty et al (2018) [1]. The FW were ground in lab mixer to get uniformity and used for solubility, hydrolysis and anaerobic biological hydrogen production experimentation, The initial characteristics of prepared FW slurry were pH 4.7 ± 0.2, TS (46.8 ± 0.58), VS/TS (95.860 ± 0.4).

Section 2. (a) Solubilization test

Carbohydrates and proteins are the main constituents of food waste, therefore the effect of Ni/Fe_2O_3-5% on food waste solubilization can be evaluated by analyzing the soluble protein and polysaccharides in the fermented liquids. The batch tests were conducted in seven groups of identical 120 mL serum bottles. Each of them was filled with synthetic medium (cellobiose 15 g/LVS), 1o% of thermochemical pretreated sludge with corresponding levels (control, 50 mg/L, 100 mg/L, 150 mg/L, 200 mg/L, 300 mg/L, 500 mg/L) of Ni/Fe_2O_3-5%. 1 mL of sock nutrient solutions were subsequently added into each bottle, then the pH in each bottle was adjusted to 6.0 ±0.2 using 3 M HCl and 3 M NaOH solutions at the beginning of each experiment, according to previous studies. All the bottles were flushed with nitrogen gas to completely remove the oxygen for over 5 min, then capped with rubber stoppers and incubated in shaker with a speed of 150 rpm and temperature of 35ºC± 2 ºC for 24 h. After incubation period, 2 mL of fermentation liquid was taken from each serum bottle to determine the concentrations of soluble protein and polysaccharides. The solubilization efficiency of protein and polysaccharides was calculated using following equation,

$$Solubilization\ efficiencies\ (\%) = C0 - C1/C0\ X\ 100\ (eq.1)$$

Section 2(b) Hydrolysis test

The solubilized carbohydrates and proteins released during solubilization stages further could be hydrolyzed into amino acids and monosaccharaides. For this analysis, Bovine Serum Protein (BSA) and Dextron were applied as model protein and carbohydrates, respectively and their hydrolysis efficiencies were investigated to assess the impact of Ni/Fe_2O_3-5% on hydrolysis stage. The operation of this experiment is the same as solubilization assay, except that 5 g/L of dextron and 5.0 g/L of BSA were also added to the synthetic medium to better characterize the hydrolysis effect. The fermentation time was carried out for 3 days. The hydrolysis efficiency of BSA and Dextron was calculated using following equation,

$$Hydrolysis\ efficiencies\ (\%) = C0 - C1/C0\ X\ 100\ (eq.2)$$

Section 2(c). Total electron transport assay

ETS was examined by performing Modified INT (2-(p-idophenyl)-3(-(p-nitrophenyl)-5-phenyltetrazolium chloride method ([2]), were performed. In brief, after 48 h of anaerobic fermentation six

set groups, the fermented samples were taken out from each serum bottles to determine the electron transporting system activity, 10 mL of culture protecting with light, then 2ml of culture and 0.5ml of 0.2% INT were added to each solution. After sealed cultures were incubated in shaker at 150 rpm, 35 for 30 min. 1 ML of 355 formaldehyde was subsequently added to terminate ETS, and mixture was centrifuged at 10000 rpm for 5 min. After that 5mL of methanol solution was added to extract iodonitrotetrazolium (INTF) by shaking at 35 for 10 min. The absorbance of supernatants was measured at 485 nm. The relative ETS activity was calculated by following the equation as, follows,

$$ETS\ activity\ (\%) = \frac{AA_{485}\ (Experiemntal)}{A_{485}\ (Control)} \times 100$$

Section 2(d) DNA extraction, Sequencing and Bioinformatics analysis

Once the DFHP system ceased, the microbial sample based on highest observed hydrogen yield from the respective reactors including 'Control' (without NPs) and Test (T-200: reactor augmented with 200 mg/L of Ni/$Fe2O_3$ -5% NPs) were subjected to comparative taxonomic and metagenomic analysis. Total DNA of both the samples were extracted and quantified using Qubit dsDNA. V4-V% region of 16sRNA of each sample was amplified using PCR. The employed methods and parameters were followed as described in literature [3]. The Sequence content Quality score across all bases observed for control and test samples is highlighted in Figure S1. Total 8.41Gb and 7.08 Gb clean data bases were observed with correspondent number of reads of 0.0562 Gb and 0.0466 for control and test samples, respectively, and data were generated which was trimmed and quality controlled through the meta WRAP-Read_Qc module [4]. The Quality score of sequences at Q20 and Q30 (%) which representing an error rate of 1 to 100, with corresponding call accuracy of 99%, table S232. As, when the sequencing quality reaches Q30, it is considered that that virtually all of the reads will be perfect, with no errors or ambiguities [5]. After filtering quality control of sequences, the contig sequences were used for metagenomic assembly. The information on the gene set for each sample set was obtained by maintaining the cluster threshold of 95% and coverage threshold of 90%. *Taxonomic annotation*: the metagenomic reads from each sample were compared against the non-reductant protein database NCBI. Bacterial diversity was estimated using microbiome package (Version 1.22.0). the function 'alpha' was used to compute the Sannon index, evenness and observed richness. Th differences in bacterial diversity between the control and test samples using Fisher-LSD non-parametric test.

Analysis and annotation of sequence output performed through metagenomics rapid annotation (MG-RAST) with the default parameters using Blast algorithm against *KEGG, eggnog, Swissport* general databases and *Crazy, BacMet CARD, GO* special databases. The KEEGG database

(https://www.genome.jp/kegg/pathway.html) includes important pathways information about the biological system n and providing a way to understand the microbial functions in host from metagenomic sets. The eggnog database: used for functional annotation based on the orthologous groups pf proteins at different taxonomic levels. Protein sequence of non-redundant genes with *CAZy* database was used to identify the carbohydrate-active enzymes in the genome. Antibiotic Resistance database was used to identify the presence of antibiotic resistance gene (ARG) using the BacMet with 80% identity cutoff [6].

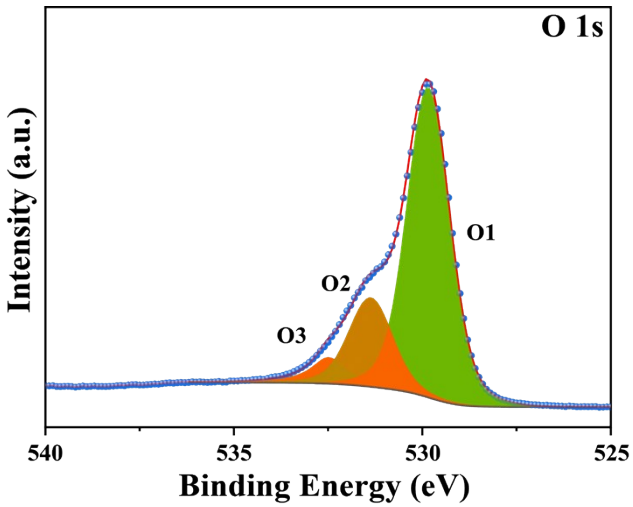

Figure S1. High resolution XPS spectrum of of oxygen from representative Ni/Fe_2O_3-5% sample

Table S1. FTIR spectrum for functional group in Food Waste

Wavenumber (cm^{-1})	Functional group	Product	Maximum peaks
4000-3000	O-H stretching vibration	H_2O	3730
3150-2700	C-H asymmetric stretching vibration	CH_4	2910
2400-2220	C=O stretching vibration	CO_2	2310
2220-2000	C-O stretching vibration	CO	2116
1900-1600	C=O stretching vibration	Aldehydes, ketones, acids	1768
1600-1480	C-C benzene skeleton stretching vibration	aromatics	1530
1480-1000	C-C, C-O benzene	Alkanes, alcohols,	1163

	skeleton stretching vibration	phenols, ethers, lipids	
780-600	C=O asymmetric stretching vibration	CO_2	637

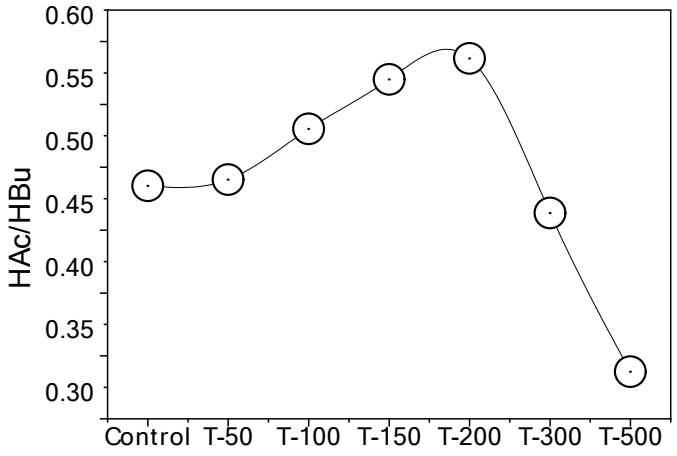

Figure S2. Effect of Ni/Fe_2O_3 to DF-system on C_2-H_{Ac}/C_4-H_{Bu} ratio.

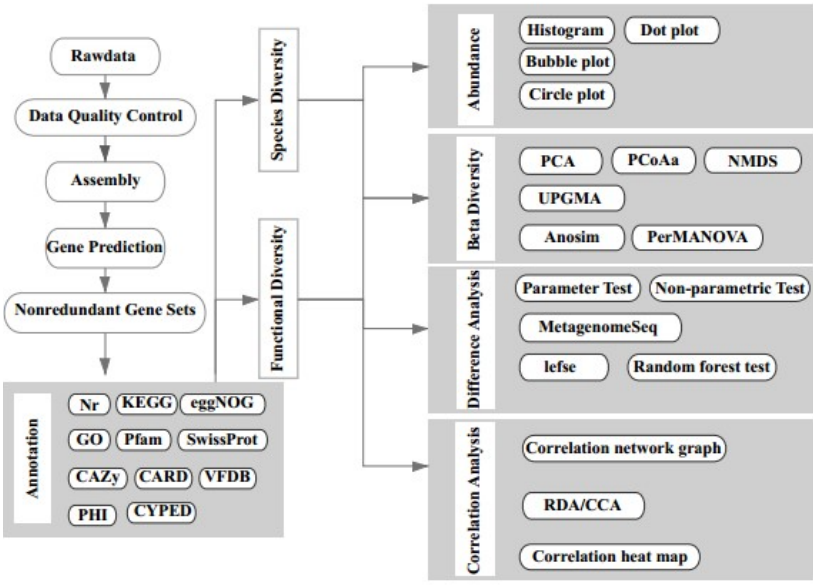

Figure S3. Flow chart followed for species and functional diversity analysis.

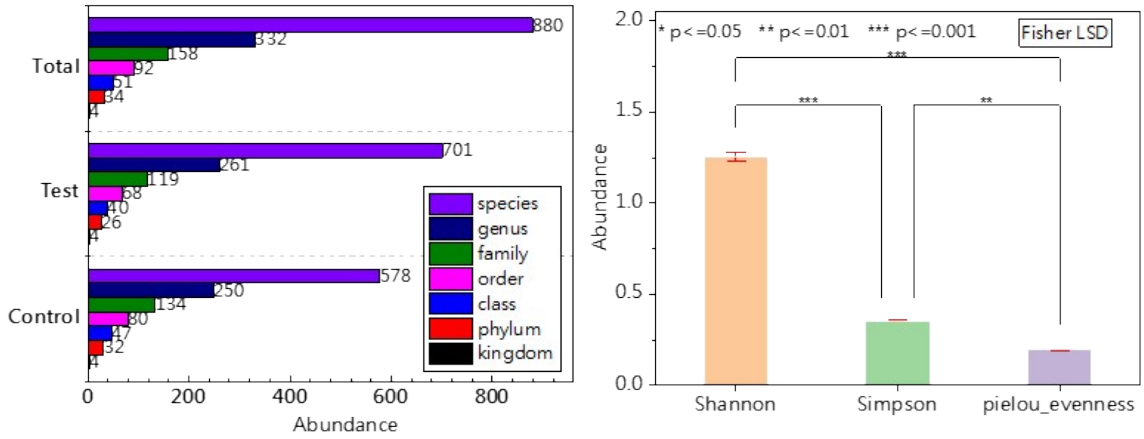

Figure S4. (a) Taxonomic diversity of microorganisms. (b) Alpha diversity regression graph

Figure S5 reflecting the taxonomic diversity in DF-sysem between control and Test, where top 20 striking variance at Phylum-level, Class-level, Order-level, Family-level, Genus-level and Species-level is highlighted. Applications of Ni/Fe_2O_3 to DF-sysem, effectively alters the taxonomic composition and diversity of the microbiome at phylum level. The presence of phylum firmicutes and proteobacteria were accounted for 97.01 % and 0.0023% for the DF-sysem added with Ni/Fe_2O_3 and, in control system it accounted for 95.24 % and 0.005%. Similar diversity was also observed at class-level where the abundancy of Clostridia and bacilli class are 95.48% and 1.18% from DF-sysem added with Ni/Fe_2O_3 and 93.15% and 1.44% for the control. The distribution of genera in DF-sysem and DF-Ni/Fe_2O_3 system were similar and clustered together. The major genera were Clostridium (91.39-93.91%), followed by Weissella, Clostridioides, and Asaccharospora, which may likely to play major role in macromolecular organic components such as starch, proteins and lipids in both the system.

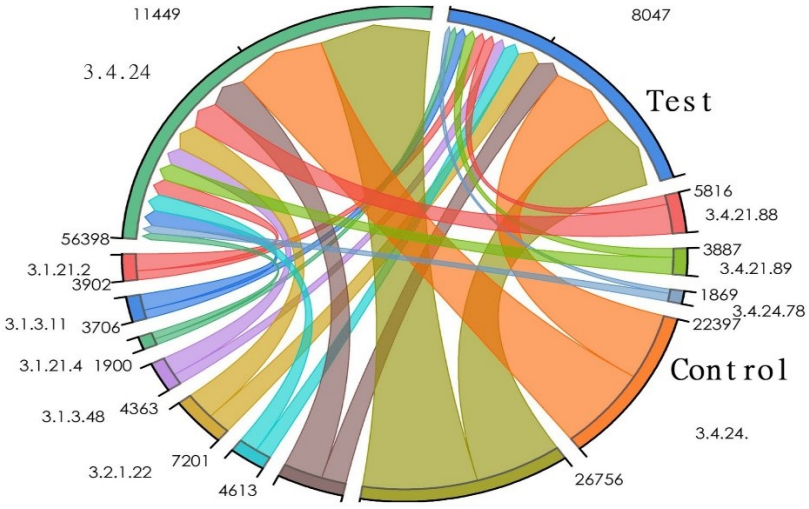

Figure S5. Abundance of Genes encoding Enzymes in Test and Control samples. EC: 3.1.X.X signified the variation in Esterase enzymes (lipases) facilitating the breakdown of phosphodiester bonds: EC: 3.2.X.X, signifies the Glycosidases facilitates the hydrolysis of O- and S- glycosylic bonds; and 3.4. X.X represents the overall protease observed in mapped gene bins.

Table SA1. Sequencing data mapping for the samples

SampleID	Clean data base(bp)	Number of Reads	GC(%)	Q20(%)	Q30(%)
Control	8411830216	56183630	30.73	99.61	98.22
Test	7082046846	46593394	31.2	99.1	96.92

Table SA2. Assembly assesses of nucleotides

Sample	Contig Num.	Total Len.(bp)	Largest Len.(bp)	N50(bp)	GC(%)	Mapped(%)
Control	32159	24098047	165584	681	39.42	96.83
Test	17386	19061807	68309	2477	35.91	97.26

Table SA3. Genetic databases

general_database	Gene number	special_database	Gene number
NR	20598	CAZy	3857
GO	7223	CARD	751
KEGG	7125	PHI-base	2309
eggNOG	15932	CYPED	508
Pfam	12272	QS	238
SwissProt	10817	BacMet	1140

Table SA4. Alpha diversity metrics

Sample	**Observed _species**	**ACE (Species richness)**	**Chao1**	**Shannon (H')**	**Simpson**	**goods_ Coverage**	**Pielou's evenness**
Test (ASM-NPs)	701	701.1875	701	1.229324	0.351003	1	0.187611291
Control (ASM)	578	578	578	1.283329	0.357152	1	0.201794866

Important annotation used in metagenomics analysis.

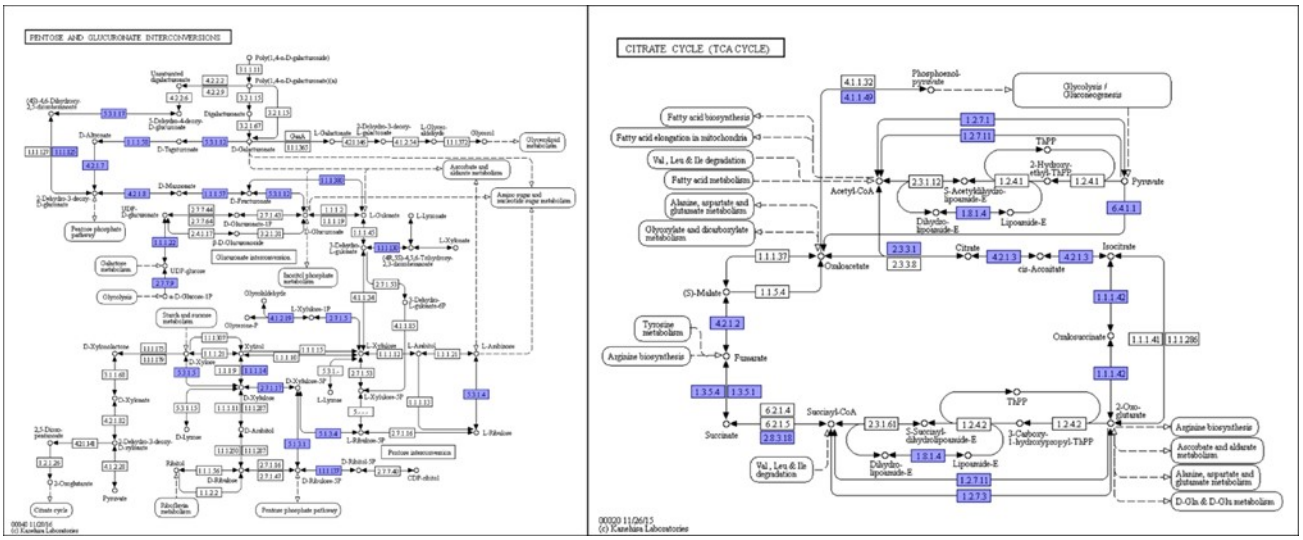

Important Genes and Enzymatic Annotations

AA1: Laccase / p-diphenol:oxygen oxidoreductase / ferroxidase (EC 1.10.3.2); ; ferroxidase (EC 1.10.3.-); Laccase-like multicopper oxidase (EC 1.10.3.-)
AA2: manganese peroxidase (EC 1.11.1.13); versatile peroxidase (EC 1.11.1.16); lignin peroxidase (EC 1.11.1.14); peroxidase (EC 1.11.1.-); cytochrome-c peroxidase (EC 1.11.1.5); ascorbate peroxidase (EC 1.11.1.11)
AA3: cellobiose dehydrogenase (EC 1.1.99.18); glucose 1-oxidase (EC 1.1.3.4); aryl alcohol oxidase (EC 1.1.3.7); alcohol oxidase (EC 1.1.3.13); pyranose oxidase (EC 1.1.3.10)
AA5: Oxidase with oxygen as acceptor (EC 1.1.3.-); galactose oxidase (EC 1.1.3.9); glyoxal oxidase (EC 1.2.3.15); alcohol oxidase (EC 1.1.3.13); raffinose oxidase (EC 1.1.3.-)
AA5: Oxidase with oxygen as acceptor (EC 1.1.3.-); galactose oxidase (EC 1.1.3.9); glyoxal oxidase (EC 1.2.3.15); alcohol oxidase (EC 1.1.3.13); raffinose oxidase (EC 1.1.3.-)
CBM2: Modules of approx. 100 residues and which are found in a large number of bacterial enzymes. The cellulose-binding function has been demonstrated in many cases. Several of these modules have been shown to also bind chitin or xylan.
CBM20: The granular starch-binding function has been demonstrated in several cases. Interact strongly with cyclodextrins. Often designated as starch-binding domains (SBD).
CBM23: Mannan-binding function demonstrated in one case.
CBM25: Starch-binding function demonstrated in one case.
CBM37: Modules of approx. 100 residues, conserved in number
ous R. albus polysaccharide-degrading enzymes and other proteins from this bacterium. Several members of CBM37 have been shown to exhibit rather broad binding specificity to xylan, chitin, microcrystalline and phosphoric-acid swollen cellulose, as well as more heterogeneous substrates, such as alfalfa cell walls, banana stem and wheat straw.
CE1: acetyl xylan esterase (EC 3.1.1.72); cinnamoyl esterase (EC 3.1.1.-); feruloyl esterase (EC 3.1.1.73); carboxylesterase (EC 3.1.1.1); S-formylglutathione hydrolase (EC 3.1.2.12); diacylglycerol O-acyltransferase (EC 2.3.1.20); trehalose 6-O-mycolyltransferase (EC 2.3.1.122)
CE3: acetyl xylan esterase (EC 3.1.1.72).

GH13: alpha-amylase (EC 3.2.1.1); pullulanase (EC 3.2.1.41); cyclomaltodextrin glucanotransferase (EC 2.4.1.19); cyclomaltodextrinase (EC 3.2.1.54); trehalose-6-phosphate hydrolase (EC 3.2.1.93); oligo-alpha-glucosidase (EC 3.2.1.10); maltogenic amylase (EC 3.2.1.133); neopullulanase (EC 3.2.1.135); alpha-glucosidase (EC 3.2.1.20); maltotetraose-forming alpha-amylase (EC 3.2.1.60); isoamylase (EC 3.2.1.68); glucodextranase (EC 3.2.1.70); maltohexaose-forming alpha-amylase (EC 3.2.1.98); maltotriose-forming alpha-amylase (EC 3.2.1.116); branching enzyme (EC 2.4.1.18); trehalose synthase (EC 5.4.99.16); 4-alpha-glucanotransferase (EC 2.4.1.25); maltopentaose-forming alpha-amylase (EC 3.2.1.-) ; amylosucrase (EC 2.4.1.4) ; sucrose phosphorylase (EC 2.4.1.7); malto-oligosyltrehalose trehalohydrolase (EC 3.2.1.141); isomaltulose synthase (EC 5.4.99.11); malto-oligosyltrehalose synthase (EC 5.4.99.15); amylo-alpha-1,6-glucosidase (EC 3.2.1.33); alpha-1,4-glucan: phosphate alpha-maltosyltransferase (EC 2.4.99.16); amino acid transporter; [retaining] sucrose 6(F)-phosphate phosphorylase (EC 2.4.1.329); [retaining] glucosylglycerol phosphorylase (EC 2.4.1.359); ; Glucosylglycerate phosphorylase (EC 2.4.1.352); [retaining] sucrose alpha-glucosidase (EC 3.2.1.48); oligosaccharide alpha-4-glucosyltransferase (EC 2.4.1.161); [retaining] alpha-amylase (EC 3.2.1.1)

GH3: beta-glucosidase (EC 3.2.1.21); xylan 1,4-beta-xylosidase (EC 3.2.1.37); beta-glucosylceramidase (EC 3.2.1.45); beta-N-acetylhexosaminidase (EC 3.2.1.52); alpha-L-arabinofuranosidase (EC 3.2.1

CE1 gene

CE1 enzymes target a large variety of substrates, however, all appear to utilize the canonical serine hydrolase mechanism, involving a catalytic triad comprising a nucleophilic serine, a histidine, and an acidic amino acid [2, 3] DOI:10.1021/bi011391c

CE3 gene

CE3 esterases catalyze the hydrolysis of O-linked acetyl groups from xylan oligo- and poly-saccharides. DOI:10.1104/pp.110.154237

Carbohydrate Binding Module Family 2

(CBM2 modules substantially potentiate the activity of cellulases and chitinsaes against purified insoluble or crystalline forms of cellulose and chitin, respectively [1, 2]. It has been proposed that cellulase-derived CBM2 modules enhance enzyme activity by increasing the local concentration or proximity of the enzyme in the vicinity of the substrate [5]. It has, however, also been reported that a CBM2 module was able to disrupt the structure of crystalline cellulose leading to enhanced enzyme activity [29]. Cell wall imaging studies have also shown that cellulose and xylan binding CBM2s enhance the activity of a pectate lyase, arabinofuranosidase and xylanases against plant cell walls [30].) (DOI:10.1042/bj3310775 | 10.1073/pnas.91.24.11383 |

GH3

Glycoside Hydrolase Family 3 currently groups together exo-acting β-D-glucosidases, α-L-arabinofuranosidases, β-D-xylopyranosidases, N-acetyl-β-D-glucosaminidases (glycoside hydrolases), and N-acetyl-β-D-glucosaminide phosphorylases [1, 2]. Widely distributed in bacteria, fungi and plants, GH3 enzymes carry out a range of functions including cellulosic biomass degradation, plant and bacterial cell wall remodeling, energy metabolism and pathogen defense. DOI:10.1016/j.chembiol.2012.09.016 | 10.1042/BJ20031028 | acceptor in the breakdown of GlcNAc-enzyme and Glc-enzyme intermediate DOI:10.1074/jbc.M114.621110 | The GlcNAc liberated during cell wall remodeling can induce cell signaling, and there are also regulatory mechanisms that are in place to coordinate the recycling of GlcNAc

with the de novo synthesis of this sugar to create UDP-GlcNAc. The release of GlcNAc during cell wall remodeling also provides opportunities for interspecies interactions, doi: 10.6064/2012/489208

GT 28 Housekeeping Genes

Relative abundance of two housekeeping genes (GT51; penicillin-binding protein and GT28; MurG transferase doi:10.1038/ismej.2013.167; MurG is an essential glycosyltransferase catalysing the last intracellular step of peptidoglycan synthesis.

References

(1) Chakraborty, D.; Karthikeyan, O. P.; Selvam, A.; Wong, J. W. Co-digestion of food waste and chemically enhanced primary treated sludge in a continuous stirred tank reactor. *Biomass and Bioenergy* **2018**, *111*, 232-240.
(2) Luo, T.; Xu, Q.; Wei, W.; Sun, J.; Dai, X.; Ni, B.-J. Performance and mechanism of Fe3O4 improving biotransformation of waste activated sludge into liquid high-value products. *Environmental Science & Technology* **2022**, *56* (6), 3658-3668.
(3) Xiu, W.; Wu, M.; Nixon, S. L.; Lloyd, J. R.; Bassil, N. M.; Gai, R.; Zhang, T.; Su, Z.; Guo, H. Genome-resolved metagenomic analysis of groundwater: insights into arsenic mobilization in biogeochemical interaction networks. *Environmental Science & Technology* **2022**, *56* (14), 10105-10119.
(4) Uritskiy, G. V.; DiRuggiero, J.; Taylor, J. MetaWRAP—a flexible pipeline for genome-resolved metagenomic data analysis. *Microbiome* **2018**, *6*, 1-13.
(5) Sun, H.-Z.; Xue, M.; Guan, L. L.; Liu, J. A collection of rumen bacteriome data from 334 mid-lactation dairy cows. *Scientific data* **2019**, *6* (1), 1-7.
(6) Pal, C.; Bengtsson-Palme, J.; Rensing, C.; Kristiansson, E.; Larsson, D. J. BacMet: antibacterial biocide and metal resistance genes database. *Nucleic acids research* **2014**, *42* (D1), D737-D743.